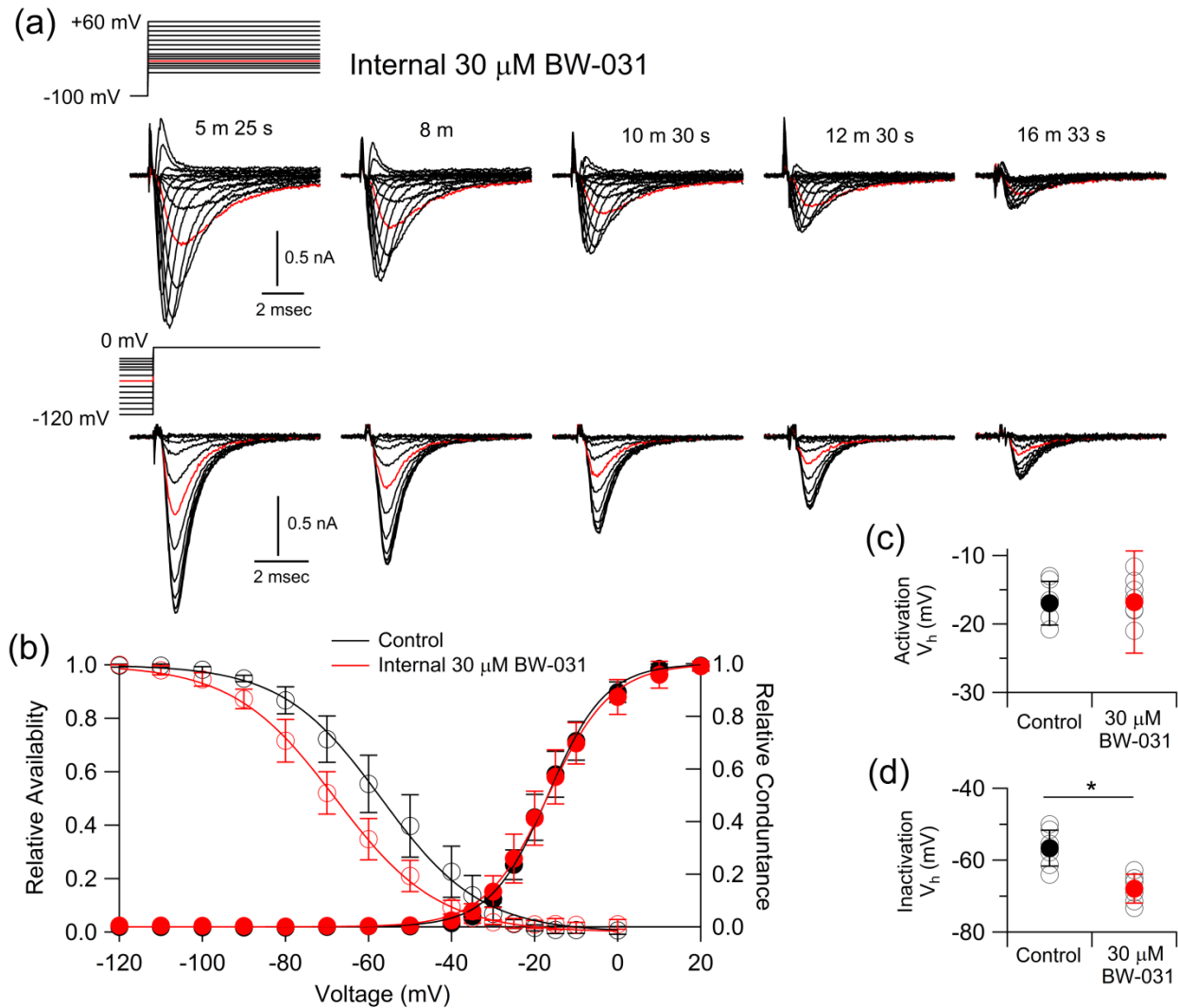


1192 **Supporting Information**

1193 **Inhibition of inflammatory pain and cough by a novel charged sodium channel blocker**

1194 Ivan Tochitsky, Sooyeon Jo, Nick Andrews, Masakazu Kotoda, Benjamin Doyle, Jaehoon Shim,  
 1195 Sebastien Talbot, David Roberson, Jinbo Lee, Louise Haste, Stephen M. Jordan, Bruce D. Levy,  
 1196 Bruce P. Bean, Clifford J. Woolf

1197



1198

1199 **Supplementary Figure 1.**

1200 Effect of intracellular 30 μM BW-031 on voltage-dependence of activation and inactivation of  
 1201 hNav1.7 channels. (a), Top, voltage-dependence of activation was determined with 50-ms steps  
 1202 from -120 mV to +60 mV delivered from a holding potential of -100 mV. Families of current  
 1203 were measured at the indicated time after establishing whole-cell configuration. Panels show first  
 1204 8 ms of test pulses from -50 to +60 (in 10 mV increments but with 5 mV increments between -40  
 1205 and -10 mV). Red traces are steps to -25 mV. Currents were corrected for leak and capacity  
 1206 currents, determined by averaged 5-mV hyperpolarizing steps from -100 mV. The last, smallest  
 1207 current traces (at 16 m 33 s) were further corrected by subtracting current in the presence of 1  
 1208 μM TTX. Bottom, voltage-dependence of inactivation determined by a 10-ms test pulse to 0 mV

1209 delivered after 50-ms conditioning pulses to voltages between -120 mV and +60 mV (activation  
1210 and inactivation determined with the same voltage protocol at the same time, with the 0 mV test  
1211 pulse for inactivation following the 50-ms steps used to determine activation). Panels show test  
1212 pulse currents at 0 mV following conditioning pulses ranging from -120 mV to -20 mV. Red  
1213 traces are for conditioning pulses to -60 mV. (b), Voltage-dependence of activation and  
1214 inactivation in cells recorded with intracellular 30  $\mu$ M BW-031 compared with interspersed  
1215 control cells recorded with BW-031-free internal solution. Voltage-dependence of activation  
1216 (filled circles) was determined by peak sodium conductance normalized to maximal peak  
1217 conductance, using a reversal potential of +45 mV. Data represent mean  $\pm$  SD. For activation:  
1218 Control, n=6; BW-031, n=8. For availability: Control, n=7; BW-031, n=6. Measurements in  
1219 BW-031 were taken when peak sodium current evoked at 0 mV from -100 mV was inhibited by  
1220 more than 50% from the initial peak current. Smooth traces drawn according to the Boltzmann  
1221 function  $1/(1+\exp(-(V-V_h)/k))$ , where  $V_h$  is the voltage of half-maximal activation,  $V$  is test  
1222 potential, and  $k$  is the slope factor. Control:  $V_h = -16.9$ ,  $k = 6.4$ . BW-031:  $V_h = -16.8$ ,  $k = 7.5$ .  
1223 Availability (open circles) was determined by peak sodium current during the test pulse to 0 mV  
1224 following 50-msec conditioning pulses, normalized to that from a conditioning pulse of -120  
1225 mV. Data fit by the Boltzmann function  $1/(1+\exp(V-V_h)/k)$ , where  $V_h$  is the voltage of half-  
1226 maximal availability,  $V$  is conditioning potential, and  $k$  is the slope factor. Control:  $V_h = -56.7$   
1227 mV,  $k = 11.4$  mV, n=7. BW-031:  $V_h = -67.9$  mV,  $k = 12$  mV, n=6. Values of  $V_h$  and  $k$  for smooth  
1228 curves in each condition were calculated as means of fits to data from individual cells. (c),  
1229 Collected values for midpoint of activation with control internal solution ( $-16.9 \pm 3.2$  mV, n=6)  
1230 and with 30  $\mu$ M BW-031 ( $-16.8 \pm 3.3$  mV, n=8). (d), Collected values for midpoint of  
1231 availability with control internal solution ( $-56.7 \pm 5.0$  mV, n=7) and with 30  $\mu$ M BW-031 ( $-67.9$   
1232  $\pm 4.0$  mV, n=6). Data represent mean  $\pm$  SD. Asterisk,  $P < 0.05$ .

1233

#### 1234 Detailed statistics for Figure data

1235 **Figure 1e:** hNav1.7 cells. Control cells with intracellular solution without compound:  $0.93 \pm 0.07$ ,  
1236 n=37. Intracellular 100  $\mu$ M BW-031:  $0.14 \pm 0.09$ , n=6. Intracellular 100  $\mu$ M QX-314:  $0.40 \pm 0.18$ ,  
1237 n=6. Extracellular 100  $\mu$ M BW-031:  $0.86 \pm 0.09$ , n=6. Comparison of intracellular 100  $\mu$ M BW-  
1238 031 with intracellular 100  $\mu$ M QX-314,  $p = 0.008$ , two-tailed Mann Whitney Test. Comparison of  
1239 intracellular 100  $\mu$ M BW-031 with extracellular 100  $\mu$ M BW-031,  $p = 0.008$ , two-tailed Mann  
1240 Whitney Test).

1241 **Figure 1g:** iPSC-derived nociceptors. Control cells with intracellular solution with no  
1242 compound:  $0.95 \pm 0.07$ , n=4. 100  $\mu$ M intracellular BW-031:  $0.13 \pm 0.09$ , n=5. 100  $\mu$ M intracellular  
1243 QX-314:  $0.43 \pm 0.15$ , n=5. 100  $\mu$ M intracellular BW-031 vs. 100  $\mu$ M intracellular QX-314,  
1244  $p = 0.01$ , two-tailed paired t-test.

1245 **Figure 2b:** Comparison of collected data by two-tailed Mann-Whitney Test. Asterisks indicate  
1246  $p < 0.05$ .

1247 **Figure 3a:** Homogeneity of variance for data was achieved by transforming raw data ( $x+1$  and  
1248 then log 10 of the new value) prior to using ANOVA. The resulting Bartlett's tests were non-  
1249 significant indicating success of the transformation method. Then 1-way ANOVA was  
1250 calculated,  $[F(3, 42) = 4.3]$ ,  $p = 0.01$ , with Tukey's post-hoc test.

1251 **Figure 3b:** 1-way ANOVA,  $[F(3, 39) = 0.33]$ ,  $p = 0.81$ .

1252 **Figure 4a:** Repeated measures two-way ANOVA with treatment as the between groups factor  
1253 and time as the within groups factor, with assumption of sphericity (Greenhouse-Geisser epsilon  
1254 value of 0.99). Treatment  $[F(2, 27) = 15]$ ,  $P < 0.0001$ ; time  $[F(2, 54) = 15]$ , and treatment x time

1255 interaction [F(4,54) = 6.8], all P<0.0001. Post-hoc Tukey's tests between treatment groups.  
1256 Treatment [F(2, 27)=15], time [F(2, 54)=15], and treatment x time interaction [F(4, 54)=6.8], all  
1257 p<0.001

1258 **Figure 4b:** Mixed-effects analysis with treatment as the between groups factor and time as the  
1259 within groups factor, with assumption of sphericity (Greenhouse-Geisser epsilon value of 1.0).  
1260 Treatment [F(1, 25)=36], time [F(6, 99)=45] and treatment x time interaction [F(6, 99)=13], all  
1261 P<0.001. Post-hoc Bonferroni tests between treatment groups at each time point.

1262 **Figure 5a:** Two-way repeated measures ANOVA with treatment as the between groups factor  
1263 and time as the within groups factor, with Greenhouse-Geisser correction for deviation from  
1264 sphericity (epsilon value of 0.63). Treatment [F(2, 27)=291], time [F(5, 135)=81] and treatment  
1265 x time interaction [F(3.2, 84.5)=81], all P<0.001. Post-hoc Tukey's tests between treatment  
1266 groups at each time point.

1267 **Figure 5b:** Two-way repeated measures ANOVA with treatment as the between groups factor  
1268 and time as the within groups factor, with Greenhouse-Geisser correction for deviation from  
1269 sphericity (epsilon value of 0.5). Treatment [F(2, 21)=225], time [F(1, 21)=225] and treatment x  
1270 time interaction [F(4, 42)=225], all P<0.001. Post-hoc Tukey's tests between treatment groups at  
1271 each time point.

1272 **Figure 5c:** Fisher's exact test (5 min time point), p=4.1x10<sup>-6</sup>.

1273 **Figure 6b:** Homogeneity of variance for data was achieved by transforming raw data (x+1 and  
1274 then log 10 of the new value), then 1-way ANOVA was calculated [F(3, 44)=5], p=0.0057, with  
1275 Tukey's post-hoc test.

1276 **Figure 7b:** Each comparison between naïve and ovalbumin-sensitized groups satisfied normality  
1277 following log 10 transformation and the transformed data were then analyzed by 2-tailed  
1278 Student's t-test.

1279 Unpaired two-tailed t-tests between naïve and ovalbumin-sensitized groups.

1280 **Figure 7c:** 1-way ANOVA, [F(3, 44)=7.1], p=0.0005; Tukey's post-hoc.

1281 **Figure 8a:** Kruskal Wallis ranks analysis.

1282 **Figure 8c:** 1-way ANOVA, [F(12, 57)=2.9], p=0.0035; Dunnett's post hoc.

1283 **Supplementary Figure 1:**

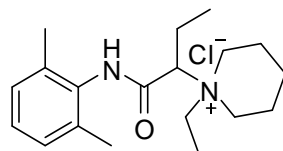
1284 Solid lines in B indicate Boltzmann equations drawn according to mean  $V_h$  and  $k$  values  
1285 calculated from fits of the Boltzmann equation to data from each cell. Activation: Control:  $V_h =$   
1286  $16.9 \pm 3.2$  mV,  $k = 6.4 \pm 0.7$  mV, n=6. BW-031:  $V_h = -16.8 \pm 3.3$  mV,  $k = 7.5 \pm 0.7$  mV, n=8.  
1287 Availability: Control:  $V_h = -56.7 \pm 5.0$  mV,  $k = 11.4 \pm 0.8$  mV, n=7. BW-031:  $V_h = -67.9 \pm 4.0$   
1288 mV,  $k = 12 \pm 0.7$  mV, n=6. Mean  $\pm$  SD. Only the midpoint of availability was statistically  
1289 significant at P<0.05 (p=0.001, unpaired Student t-test) between data from cells with control or  
1290 BW-031-containing internal solution.

1291

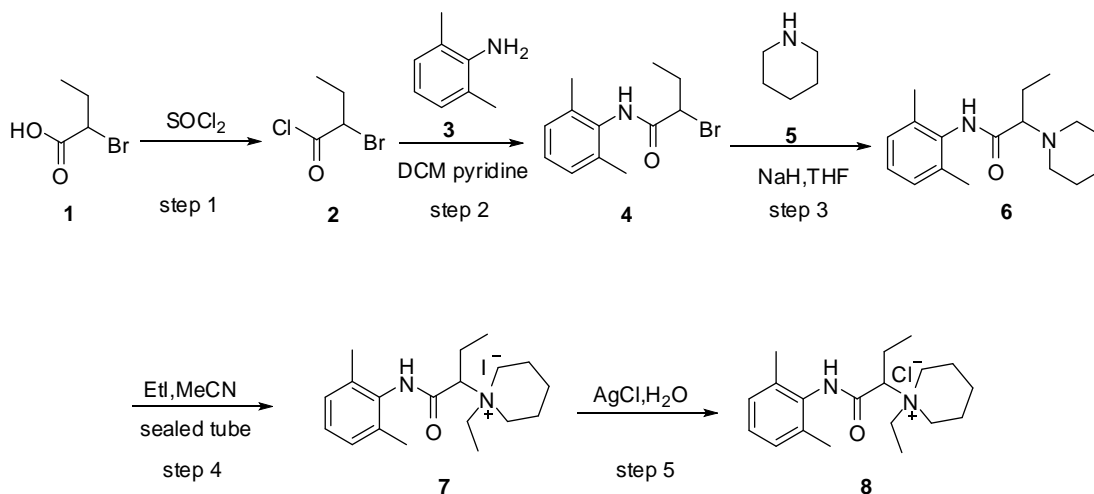
1292

1293  
1294

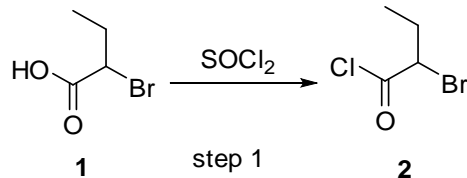
## Synthesis of BW-031 (1-(1-(2, 6-dimethylphenylamino)-1-oxobutan-2-yl)-1-ethylpiperidinium)



### Synthetic Scheme

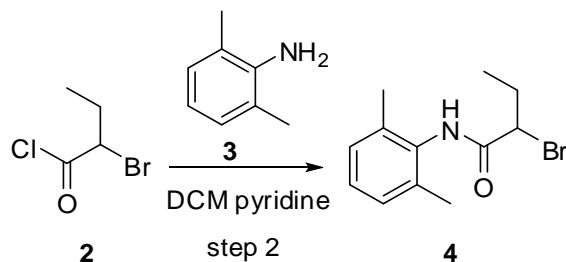


#### Step 1: Preparation of intermediate 2



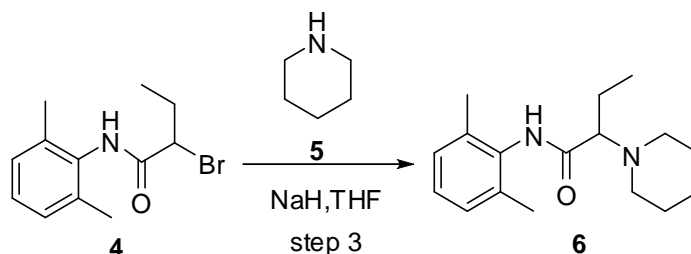
To a mixture of **1** (10.0g, 59.88mmol) was added  $\text{SOCl}_2$  (60mL,  $c=1.0$ ). The mixture was heated to reflux. After completion, the reaction mixture was concentrated under reduce pressure to give intermediate **2** (9.2g, yield=82.8%) as a yellow oil.

#### Step 2: Preparation of intermediate 4



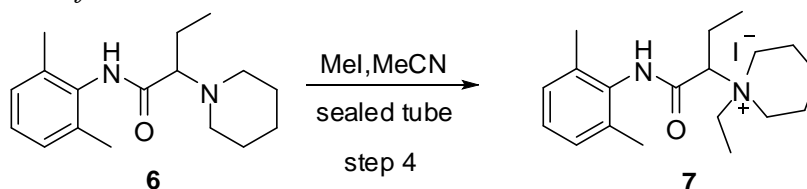
To a solution of **3** (5.0g, 41.3mmol, 1.0eq) in DCM (100ml,  $c=0.5$ ) was added pyridine (4.9g, 61.95mmol, 1.5eq). To the solution was added **2** (9.2g, 49.59mmol, 1.2eq) in DCM (40mL,  $c=1.2$ ). The reaction mixture was stirred at room temperature overnight. Then to the solution was added water (50mL). The organic phase was washed with brine, dried over  $\text{Na}_2\text{SO}_4$ , filtered and concentrated under reduce pressure. The residue was washed with n-hexane to give intermediate **4** (7.8g, yield=70%, HPLC: 98.6%).

*Step 3: Preparation of intermediate 6*



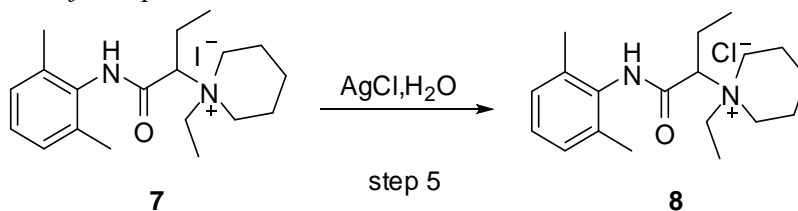
To a solution of NaH (0.35g, 14.8mmol, 2.0eq) in THF (37mL, c=0.4) was added **5** (0.75g, 8.8mmol, 1.2eq). To the solution was added **4** (2.0g, 7.4mmol, 1.0eq) in THF (20mL, c=0.37). The reaction mixture was then stirred at room temperature overnight. To the suspension was added water (20mL) and EA (50mL). The organic phase was washed with water (50mL×2). Then the organic phase was adjusted to pH 2, extracted with EA(40mL×2). The aqueous fractions were combined and adjusted to pH 9, then extracted with EA (40×2). The combined organic fractions were washed with brine, dried over Na<sub>2</sub>SO<sub>4</sub>, filtered and concentrated under reduce pressure. The residue was washed with n-hexane to give the intermediate **6** (0.48g, yield=24%, HPLC: 99.3%) as a solid.

*Step 4: Preparation of intermediate 7*



Intermediate **6** (0.48g, 1.75mmol, 1.0 eq) and MeCN (9mL, c=0.2) was added in sealed tube. To this solution, EtI (2mL, 14.0 eq) was added. After addition, the reaction mixture was stirred at 90°C for 10h. After completion, the reaction mixture was concentrated under reduce pressure. The residue was purified by column chromatography to give intermediate **7** (470mg, yield=62.6%, HPLC: 99%) as a solid.

*Step 4: Preparation of compound 8*



1295 To a solution of **7** (200mg, 0.465mmol, 1.0 eq) in deionized water (3ml, c=0.15) was added  
1296 AgCl (133mg, 0.93mmol, 2.0 eq). After addition, the reaction mixture was stirred at room  
1297 temperature overnight. The suspension was then filtered and the filtrate was lyophilized to give  
1298 compound **8** (141mg, yield=89.8%) as a solid. HPLC purity: at 220nm; Mass: M+1=339.4. 1H  
1299 NMR (300 MHz, D<sub>2</sub>O): δ 7.117 (m, 3H), 4.056 (dd, J=8.1 Hz, 1H), 3.712~3.808 (m, 1H), 3.656  
1300 (m, J=13.2 Hz, 2H), 3.510~3.582 (m, 1H), 3.344 (m, 2H), 2.117 (s, 6H), 1.984~2.070 (m, 2H),  
1301 1.818 (m, 4H), 1.660 (m, 1H), 1.455 (m, 1H), 1.278 (t, J=7.2 Hz, 3H), 1.107 (t, 3H) ppm.